

Cuticular Photophores of Two Decapod Crustaceans, *Oplophorus spinosus* and *Systellaspis debilis*

M. S. NOWEL^{1,*}, P. M. J. SHELTON², AND P. J. HERRING³

¹*Department of Biology, Providence College, Providence, Rhode Island 02918-0001;* ²*Department of Biology, School of Biological Sciences, University of Leicester, Leicester LE1 7RH, UK; and* ³*Southampton Oceanography Centre, Empress Dock, Southampton SO14 3ZH, UK*

Abstract. The organization, ultrastructure, growth, and development of two types of cuticular photophore in oplophorid shrimps (*Oplophorus spinosus* and *Systellaspis debilis*) are described. Photophores located in the third maxilliped consist of a unit structure comprising a single photocyte and associated pigment cells. Reflecting pigment cells contain white pigment and form an apical cap above the photocyte; sheath cells contain red carotenoid pigment and form a light-absorbing layer around the photophore. Photophores located on the pleopods are compound structures comprising many photocytes. They also contain the same types of pigment cell that are found in the unit photophores of the maxilliped. Paracrystalline bodies at the apical ends of the photocytes in both types of photophore are thought to be associated with light generation. Both types of photophore have mechanisms for tilting in the pitch plane. In the maxilliped, the apices of the photophores are connected to a ligament that has its origin in the propodus. Flexion or extension of the dactylus displaces the ligament, which tilts the photophores synchronously. The cuticular window beneath each photophore remains stationary. The tilt mechanism of the pleopod photophores is quite different, and depends upon muscular contraction. A main and an accessory longitudinal muscle cause backwards rotation of the photophore by deforming the cuticle surface. A loop muscle that passes around the anterior face of the photophore causes forward rotation. The two mech-

anisms optimize the use of the photophores in ventral camouflage. They allow photophore rotation to compensate for changes in the shrimp's orientation in the plane of pitch and thus maintain the ventral direction of the luminescence.

Introduction

Many groups of oceanic animals are bioluminescent (Harvey, 1952; Herring, 1978). In a number of these, the luminescence is produced in single cells or groups of cells without any other associated structures. However, in some animals the bioluminescent cells (photocytes, the "photogenic cells" of Dennell, 1940) are part of a complex organ (photophore) whose additional features may modify the direction, intensity, spectral distribution, or angular distribution of the emitted light (Denton *et al.*, 1972, 1985; Herring, 1985a). In the sea, such photophores are restricted to fish, cephalopods, euphausiids, and decapod crustaceans, and are particularly common in members of the mesopelagic fauna, whose normal daytime depth distribution is between 200 m and 1000 m. These animals tend to direct their luminescence downwards, and the photophores are most numerous along the ventral surface, where their function is primarily that of counterillumination. They camouflage the animal by emitting bioluminescence whose characteristics closely match those of the downwelling light. This eliminates the silhouette that would otherwise be visible from below. In euphausiid shrimps, the ventral directionality is further maintained during swimming by rotating the photophores in response to changes in body tilt (Hardy, 1962, 1964; Land, 1980; Grinnell *et al.*, 1988).

Received 17 June 1998; accepted 31 August 1998.

* To whom correspondence should be addressed. E-mail: mnowel@providence.edu

Among the decapod shrimps, several families of both the Penaeidea and Caridea have such photophores, and they may be formed either as cuticular structures or as modified hepatopancreas tubules (Herring, 1976, 1985b). In the caridean family Oplophoridae, whose species range in depth distribution from the upper mesopelagic to the deep-sea floor, the two shallowest genera—*Systellaspis* and *Oplophorus* (the latter here including the genus *Janicella*)—have many cuticular photophores. These are present on the eyes, limbs, cephalothorax, and abdomen. They take various forms, but in live animals all except those on the pleopods appear to be made up of variable-sized groups of very similar small units. Those on the third maxilliped represent the simplest level of organization, consisting of single photophore units each containing a single photocyte. At the other extreme, the abdominal photophores on the protopodite of each pleopod contain many photocytes that are less obviously composed of multiple units. The morphology of the photophores from various sites on a number of species has been described by Coutière (1905, 1906), Kemp (1910a, b), and later by Dennell (1940, 1942, 1955). Dennell (1940) interpreted his results as evidence for a range of photophore types both within and between species of *Systellaspis* and *Oplophorus*.

In this paper we reexamine some of this apparent variation and conclude that the different appearances of the photophores reflect different degrees of aggregation and merging of fundamentally similar units. We describe the ultrastructure of a typical unit in the maxilliped and the compound nature of the pleopod photophores. We also report the rotation of some of the photophores in the plane of pitch and the anatomical means whereby this is achieved. Similar rotation of some counterilluminating photophores has been described in the thoracic and abdominal photophores of euphausiids, as noted above, and in the hepatic photophores of species of the penaeidean shrimp *Sergestes* (Latz and Case, 1982).

Materials and Methods

Specimens were collected during cruises 195 (1990) and 204 (1993) of RRS *Discovery* in the eastern North Atlantic, between the Canary and Cape Verde Islands. They were taken from depths of up to 600 m, using the RMT 1 + 8 net system (Roe and Shale, 1979). The use of a closing cod end (Wild *et al.*, 1985) maintained the shrimps in good condition. They were processed on board ship. Juvenile and adult specimens were fixed in Karnovsky's (1965) fixative, and most were postfixed in 1% phosphate-buffered osmium tetroxide at pH 7.4. Specimens were dehydrated in a graded acetone series and embedded in either Spurr's resin or in Araldite. On shore, semithin (1 μ m) sections were cut on a Huxley Cambridge

ultramicrotome, mounted on subbed slides (0.1% gelatine; 0.01% chrome alum), and stained with toluidine blue (1% in 1% borax). Ultrathin sections were collected on uncoated grids or on 0.5% pioloform films that were mounted on slot grids; they were stained with aqueous uranyl acetate and lead citrate and examined using a JEOL 100 CX electron microscope (JEOL Ltd, Colindale, London, UK). Light micrographs were taken on Pan F film with a Zeiss Photomicroscope II.

Results

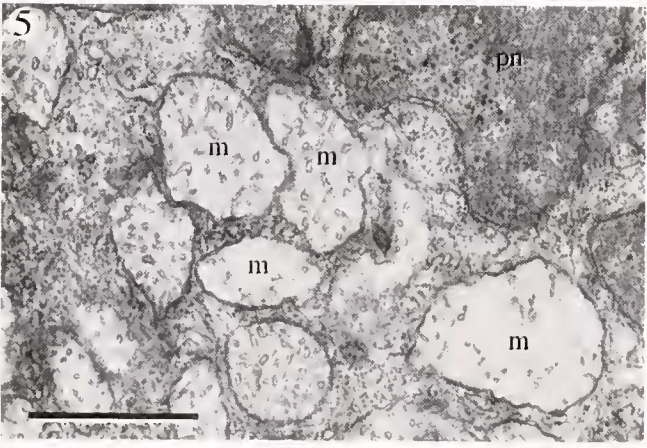
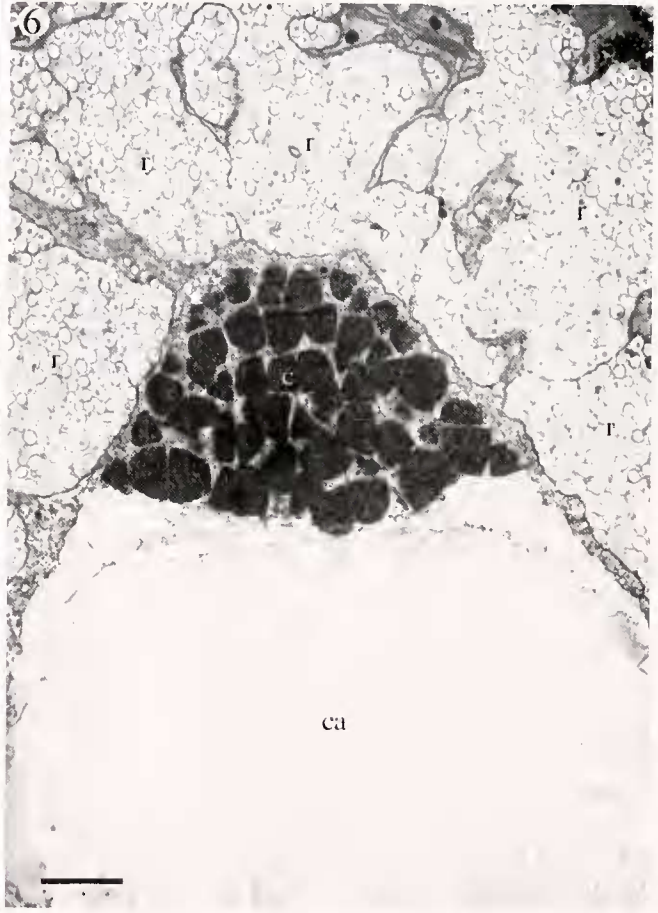
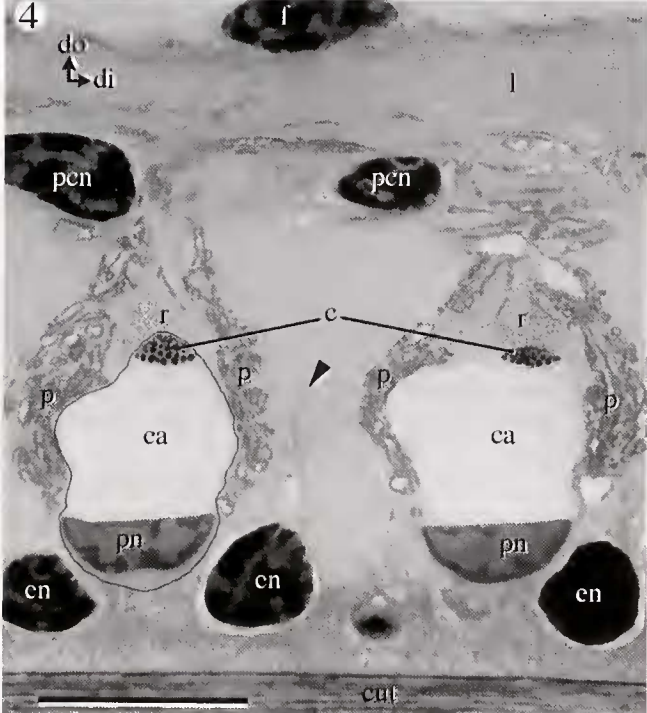
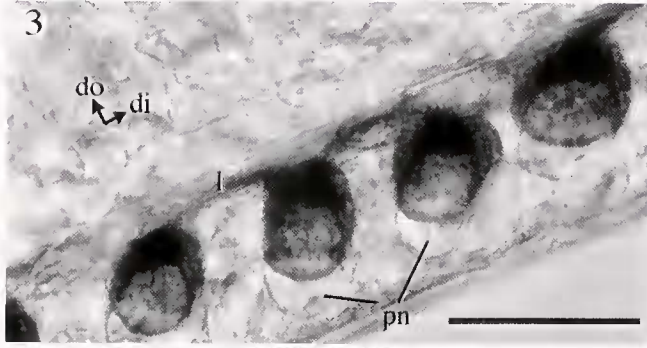
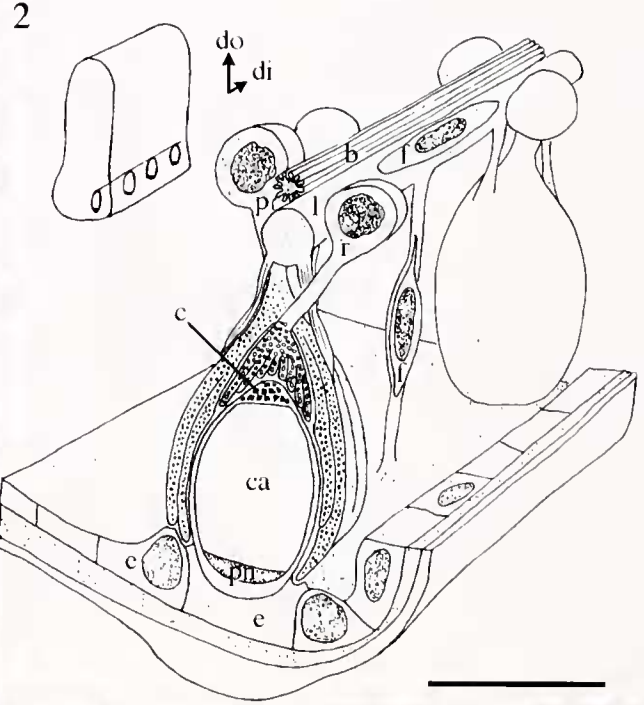
The 3rd maxilliped photophores

The photophores in the dactylus of the 3rd maxilliped are located along its posterior (ventral) surface towards the lateral edge, and they are organized in a single row (Fig. 1). There is a group of relatively large photophores located at the very tip. These are always separate from the main row, are present in the earliest postlarvae, and are among the first to develop. From this distal group the photophore row extends proximally to the joint. In older individuals, both the proximal and distal ends of this row are several photophores wide. We selected this group of photophores in *Oplophorus spinosus* as representative of the basic subunits. We chose these photophores because they are easily visible in the transparent dactylus of juvenile specimens, are not obscured by pigment as in *Systellaspis debilis*, and are organized in a largely linear array that allows their developmental sequence to be readily determined in live animals. At most other sites, the individual subunits are obscured by pigment or by the two-dimensional nature of the arrays.

The photophores of the 3rd maxilliped represent the simplest grade of photophore organization, and their overall structure is summarized in Figure 2. They are ovoid to conical and consist of a single photocyte and two types of pigment cell. In fresh specimens, the clear nucleus of the photocyte can be seen at its basal, most ventral (closest to the cuticle) end (Fig. 3). Its refractile properties suggest that it may have an optical function. This basal end of the photophore is attached to a specialized region of the epidermis. At the dorsal end, the apex of the photophore is connected to a ligament extending the length of the dactylus (Figs. 2 and 3).

The photocyte

The photocyte is more or less ovoid, and electron micrographs reveal its close association with the epidermis (Fig. 4). When treated with uranyl acetate and lead citrate, its nucleus stains lightly compared with those of nearby epidermal cells. In addition, the chromatin is concentrated around the periphery of the nucleus. The shape of the nucleus is plano-convex, with the curved face directed



ventrally towards the limb surface. In *O. spinosus*, there is a dimple in the convex surface, but in *S. debilis* there is not. The shape and distinctive staining properties of the nucleus may relate to its presumed refractive function.

Most of the volume of the photocyte is occupied by a single clear vacuole lacking organelles or inclusions but filled with a material that sometimes shows a very fine granulation (Fig. 6). Dennell (1940) calls this the "clear area" of the "photogenic cell." The rest of the cytoplasm is located at the periphery of the cell and contains cytoskeletal elements, mitochondria, vesicles, and paracrystalline bodies.

The basal cytoplasm of the mature photocyte, ventral to the nucleus (and in *O. spinosus*, extending into its dimpled face) is packed with mitochondria (Fig. 5); in all other regions, the cytoplasm surrounding the clear central region of the cell is devoid of these organelles. The cytoplasm at the apex of the cell, lying above the clear area, contains numerous osmiophilic paracrystalline bodies (Figs. 4 and 6). These bodies are membrane-bound structures stacked into a flat cone in the most apical region of the cell. They usually have flat sides and occur in a range of shapes. Many appear rhomboidal or square while others are triangular in section. In all cases, they have a regular, square lattice substructure, with a periodicity of about 14.8 nm (SD = 0.36 in 15 measurements) (Fig. 7). Cytoplasmic processes arising from the apical region of the photocyte extend into the surrounding reflecting pigment cell processes (Fig. 6). The cytoplasm in the apical

region of the photocyte and the processes arising from it contain microfilamentous cytoskeletal elements.

The pigment cells

Two distinct types of pigment cell contribute to each photophore. In fresh tissue, one type has a broadband white reflectance. The other is scarlet, and the pigment has the typical characteristics of the carotenoid astaxanthin and its esters, which are responsible for most of the animal's color (Herring, 1973). The somata are associated with the ligament dorsal to the row of photophores (Figs. 2 and 4). These somata contain abundant rough endoplasmic reticulum. Cytoplasmic processes that contain most of the pigment granules extend ventrally from the somata.

In material sectioned for light and electron microscopy, the processes containing the white pigment granules form a cap around the apex of each photocyte (Fig. 6). These processes contain relatively uniform, densely packed membrane-bound pigment granules measuring up to about 0.40 μm in diameter in *O. spinosus* and up to about 0.25 μm in diameter in *S. debilis*. The granules contain electron-lucent material around a central core of moderately dense material. There are similarities between the contents of these pigment granules and those of the tapeta of various crustacean eyes (shrimps: Doughtie and Rao, 1984, and Ball *et al.*, 1986; crayfish: Piekos, 1986; lobsters, Shelton *et al.*, 1986), which is evidence for their role as a reflecting layer. The cytoplasm of the reflecting

Figures 1–6. Views of maxilliped photophores in *Oplophorus spinosus*.

Figure 1. Light micrograph of a lateral view of a maxilliped, showing the photophores arranged in a row along the ventral face of the dactylus with a pair of large photophores at the distal tip (arrow). Note the immature photophores within the row (arrowheads). di, distal; do, dorsal; l, ligament. Scale bar: 300 μm .

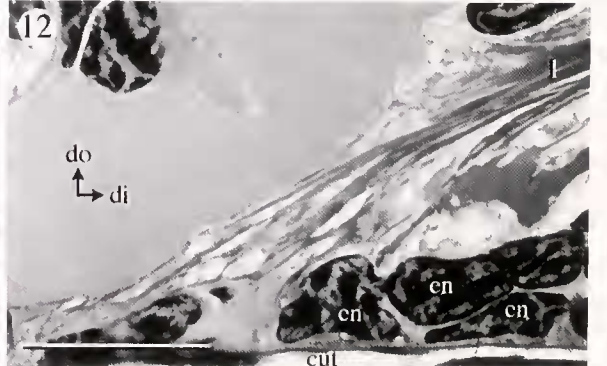
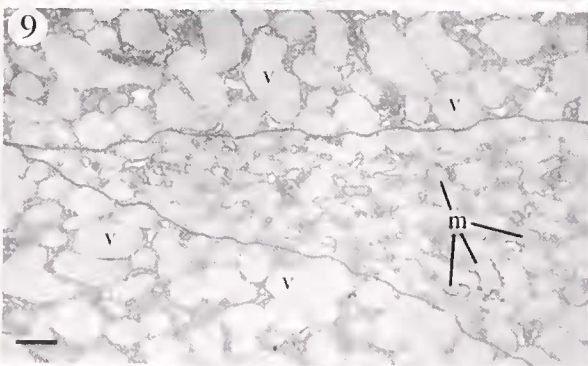
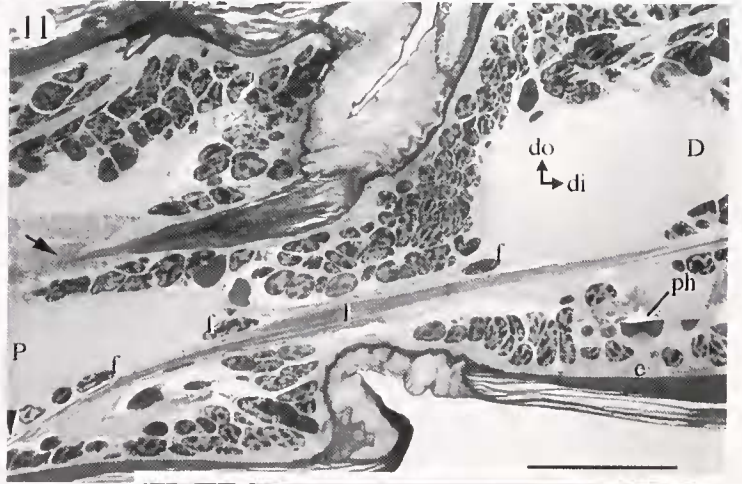
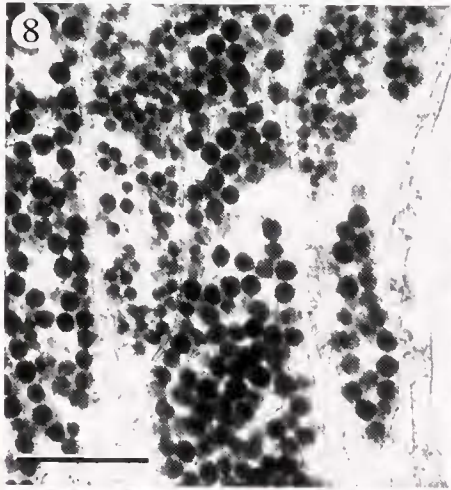
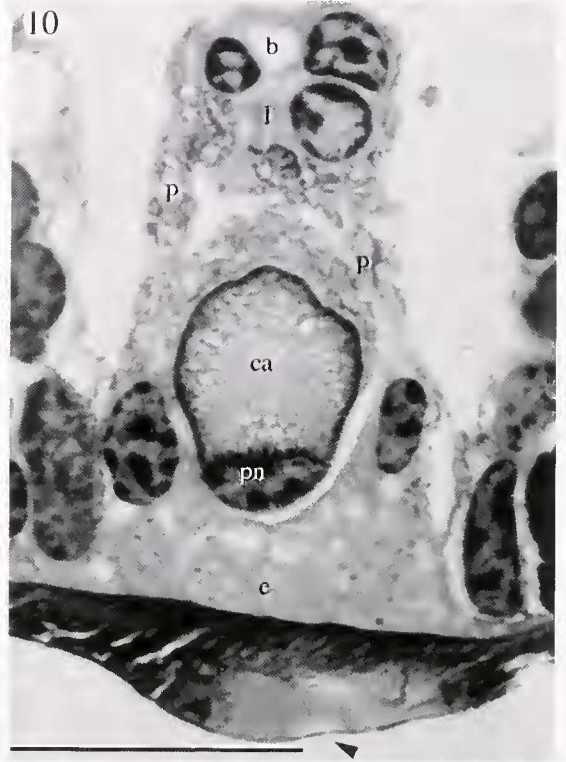
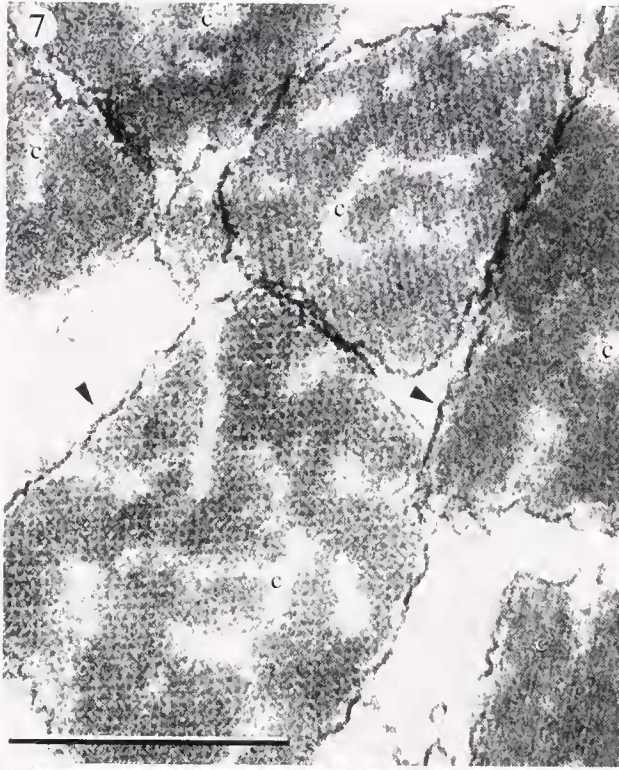
Figure 2. Semi-schematic drawings of portions of the maxilliped to show the arrangement of the photophores lined along the ventro-lateral portion of the dactylus (upper), and the cellular organization of two photophores (lower). Each photophore consists of a photogenic cell with a nucleus (pn) at the base and paracrystalline bodies (c) at the apex; a cap of processes of a reflecting pigment cell (r); and a sheath of processes of carotenoid pigment cells (p). A ligament (l) composed of extracellular fibrils formed by fibroblasts (f) joins the photophores to each other and anchors them to the "window" epidermis (e) below. A blood vessel (b) runs parallel to and above the ligament. di, distal; do, dorsal. Dimensions are approximate. Scale bar: 40 μm .

Figure 3. Light micrograph of a lateral view of the ventral portion of the maxilliped. The ligament (l) is attached to the apex of each photophore. Note the clear, lens-shaped photocyte nuclei (pn). di, distal; do, dorsal. Scale bar: 75 μm .

Figure 4. Light micrograph of a longitudinal section through the maxilliped showing two photophores oriented perpendicular to the cuticular surface. One photocyte is outlined to indicate its boundaries with the "window" epidermal cells. Each photocyte has a lens-shaped nucleus (pn) at its base and an array of paracrystalline bodies (c) above a clear area (ca). The apex of the photocyte is connected to the ligament (l) by a cap of reflecting pigment cell processes (r) and a sheath of carotenoid pigment cells (p). Fibrous strands (arrowhead) extend from the ligament alongside the photophores. cut, surface cuticle; di, distal; do, dorsal; en, "window" epidermal cell nuclei; f, fibroblast; pen, pigment cell nucleus. Scale bar: 40 μm .

Figure 5. Electron micrograph of the basal cytoplasm of the photocyte of the maxilliped photophore showing abundant mitochondria (m) which lie below the nucleus (pn). Scale bar: 1 μm .

Figure 6. Electron micrograph of a section through the apex of a photocyte and the cap of reflecting pigment cell processes (r). c, paracrystalline bodies; ca, clear area. Scale bar: 2 μm .



cell also contains some mitochondria but few other organelles.

Numerous abutting processes of the carotenoid pigment cells surround the photocyte and its associated reflecting cap down to its junction with the epidermis. They contain many electron-dense pigment granules that do not appear to be membrane-bound and resemble those in crustacean chromatophores (Elofsson, 1971). The size of the granules is relatively uniform up to a diameter of about $0.15\ \mu\text{m}$ in *O. spinosus* (Fig. 8) and $0.25\ \mu\text{m}$ in *S. debilis*. As with the reflecting pigment cells, the granules are contained in numerous abutting cytoplasmic processes. The presumed function of the carotenoid pigment is to prevent lateral leakage of light from the photophore.

The underlying epidermis and cuticle

The photophores lie on a strip of a specialized "window" epidermis through which light generated by the photophore is transmitted (Fig. 4). This epidermis is composed of a single layer of epithelial cells in which the cytoplasm is filled with electron-lucent droplets and a few mitochondria (Fig. 9). There is an abrupt transition between the window epidermis and the general cuticular epidermis. The latter contains abundant rough endoplasmic reticulum that gives its cytoplasm a somewhat more electron-dense appearance. The clearly differentiated nature of the window epidermis may relate to the optical requirements of the photophore structure.

The cuticle secreted by the window epidermis differs in two ways from that secreted by the non-photophore epidermis. In both *S. debilis* and *O. spinosus*, the "window" cuticle is thicker than that which surrounds it. In *S. debilis*, the window cuticle ventral to the row of photo-

phores is formed into a lens-like ridge (Fig. 10) that is probably of optical significance; *O. spinosus* has no such obvious ridge. In fresh preparations of both species, the window cuticle has a distinct blue color with an absorption maximum around 560 nm in *O. spinosus* and 530 nm in *S. debilis* (P.J.H., unpub. data), whereas the surrounding cuticle does not. This color is visible over the pleopod photophores in the first zoeas of *S. debilis*, but develops only in later stage larvae of *O. spinosus*.

The ligament

With the exception of the separate group of larger photophores at the distal end of the dactylus, each photophore along the length of the maxilliped is attached to a ligament lying dorsal to the row (Figs. 2, 3, and 4). The ligament arises at the distal end of the propodus (Fig. 11), where it is attached directly to the cuticular epidermis (Fig. 12). It extends to the most distal of the photophores in the main row, but not as far as the large photophores of the terminal group. The ligament consists of thick bundles of fibrils that are parallel to the long axis of the limb. These fibrils have a diameter of 20 nm, and a periodicity of about 9.7 nm (SD = 0.52 in ten measurements) along their length (Figs. 13 and 14). They are associated with fibroblasts distributed along the ligament and are assumed to be formed by them (Figs. 4 and 11).

Smaller bundles of fibrils extend ventrally from the ligament to the apex of each photophore (Figs. 4 and 15). These bundles are found amidst the processes of the pigment cells and in between adjacent photophores at all levels down to the window epidermis. Like the thicker bundles, these are associated with fibroblasts (Fig. 15) and serve to connect each photophore to the ligament or

Figures 7–10. Micrographs of maxilliped photophores; all except Fig. 10 are of *Oplophorus spinosus*.

Figure 7. Electron micrograph of the membrane-bound (arrowheads) paracrystalline bodies (c) of the photocyte showing the square lattice substructure. Scale bar: $0.5\ \mu\text{m}$.

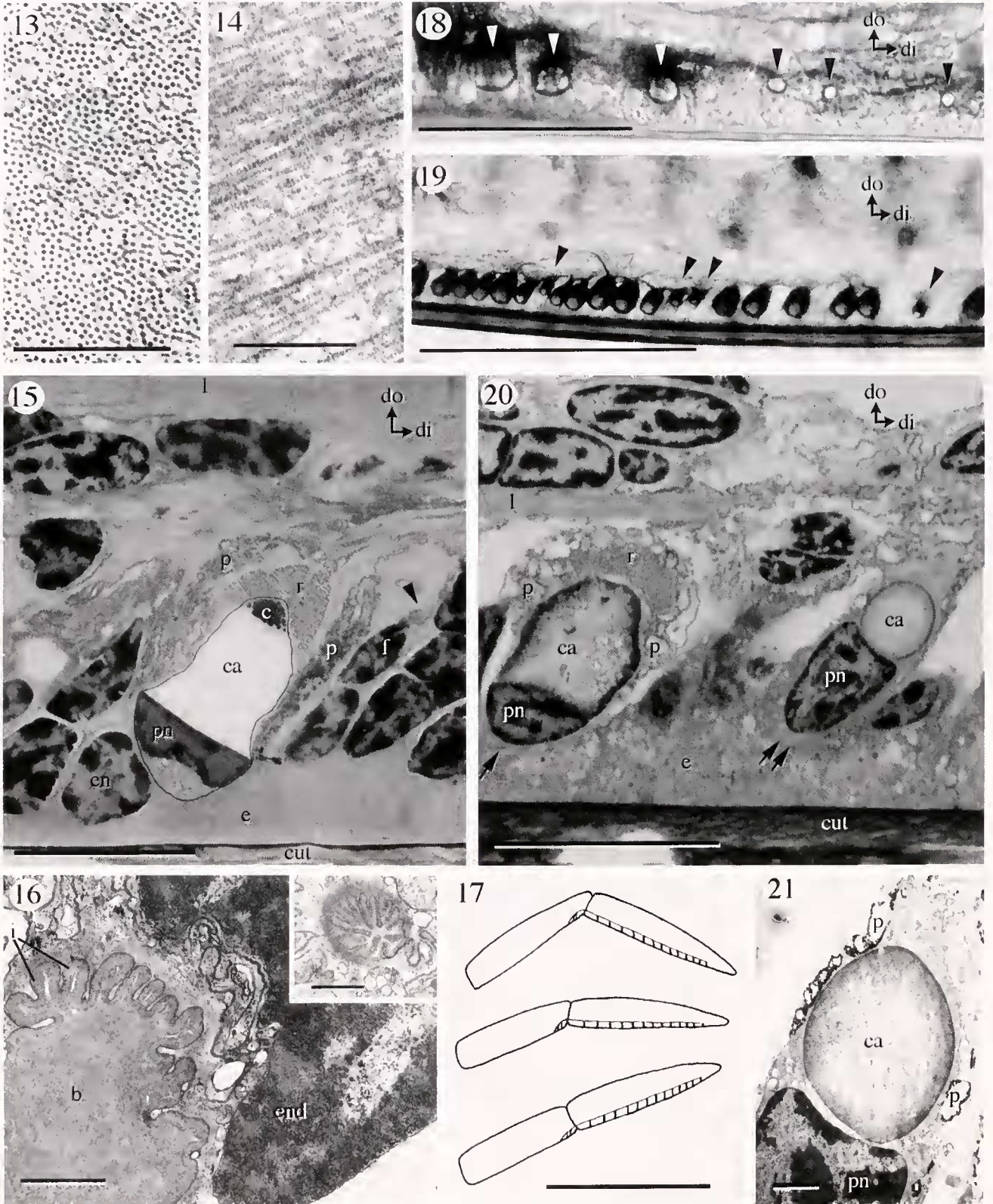
Figure 8. Electron micrograph showing the processes of a carotenoid pigment cell that form a sheath around the photophore. Scale bar: $1\ \mu\text{m}$.

Figure 9. Electron micrograph of a horizontal section through the "window" epidermis of the maxilliped. Note the abundance of membrane-bound vesicles (v), with minimal cytoplasm between them, and the relatively few mitochondria (m). Scale bar: $1\ \mu\text{m}$.

Figure 10. Light micrograph of a section through a photophore in the maxilliped of *Systellaspis debilis*, showing the similarities with those of *O. spinosus*. The photocyte lies above the "window" epidermis (e). The ligament (l), blood vessel (b), and processes of the pigment cells (p) can be seen above the photocyte. In *S. debilis*, the photocyte "clear area" (ca) is invariably filled with an electron-dense material. Note that the cuticle below the simple photophore has a convex lens-like contour (arrowhead). pn, photocyte nucleus. Scale bar: $40\ \mu\text{m}$.

Figure 11. Light micrograph of a longitudinal section through the propodus (P) and dactylus (D), of the maxilliped. The most proximal of the row of photophores (ph) in the dactylus is shown. The insertion of the ligament (l) into the epidermis of the propodus is indicated (arrowhead), as well as the insertion of the flexor muscle to the cuticle of the joint (arrow). di, distal; do, dorsal; e, window epidermis; f, fibroblast. Scale bar: $100\ \mu\text{m}$.

Figure 12. High-power light micrograph showing the attachment of the ligament fibers (l) to the epidermis of the propodus. cut, cuticle; di, distal; do, dorsal; en, epidermal cell nuclei. Scale bar: $40\ \mu\text{m}$.



the ligament to the epidermis between adjacent photophores.

A prominent blood vessel runs the whole length of the ligament, along its dorsal surface. This vessel exhibits a folding of its internal intima and endothelial lining (Figs. 2 and 16), which would facilitate any changes in its diameter. Similar blood vessels have been found in other crustacean systems (Peterson and Loizzi, 1974; Schönenberger, 1977; Martin and Hose, 1992). Capillaries extend from the main blood vessel toward the photophore; these, too, have folded walls (Fig. 16 inset).

Tilt control of the maxilliped photophores

The ligament that is attached to all but the terminal group of photophores in the dactylus appears to have a role in determining their orientations. Examination of fresh and fixed whole-mount preparations and of the longitudinally sectioned dactylus shows that in any one specimen, all the photophores in the main row are oriented

in the same way. However, the orientation varies from specimen to specimen: in some cases they are perpendicular to the surface of the maxilliped (Fig. 4); in others they are tilted (Figs. 15, 20, and 22). The ligament provides the means whereby such changes of orientation occur.

Owing to its origin in the ventral region of the distal propodus, the ligament and the apices of all the photophores connected to it are pulled proximally, with respect to the dactylus, by flexion of the propodus/dactylus joint. Extension of the joint results in distal movement of the ligament and the apices of the photophores connected to it. The photophores are fixed to the integument at their basal surfaces, so these ligament displacements cause them to tilt (Fig. 17).

Because most of our observations were made on preserved material, we have not been able to describe the precise relationship between joint angle and photophore tilt. Nevertheless, one of us (P.J.H.) was able to confirm that in fresh material the photophores do indeed tilt as the dactylus is rotated with respect to the propodus. A

Figures 13–21. Views of maxilliped photophores of *Oplophorus spinosus* (Figs. 13–19) and *Systellapsis debilis* (Figs. 20, 21).

Figure 13. Electron micrograph of a transverse section through the ligament dorsal to the maxilliped photophores showing the dense packing of the fibrils. Scale bar: 0.25 μm .

Figure 14. Electron micrograph of a longitudinal section through the ligament of the maxilliped showing the highly oriented fibrils. Scale bar: 0.25 μm .

Figure 15. Light micrograph of a longitudinal section through the maxilliped showing the photophore tilted proximally. The photocyte has been outlined to show its boundaries. c, paracrystalline bodies of photocyte; ca, clear area of photocyte; cut, cuticle; di, distal; do, dorsal; e, "window" epidermis cytoplasm; en, "window" epidermis nucleus; f, fibroblast (with arrowhead indicating fibers extending toward ligament); l, ligament; p, carotenoid pigment cell processes; pn, nucleus of photocyte; r, reflector pigment cell processes. Scale bar: 40 μm .

Figure 16. Electron micrograph of a transverse section of the blood vessel (b) associated with the ligament of the maxilliped. The wall of the blood vessel is a folded structure comprising an endothelial cell and an internal intima (i). The inset shows a capillary that has branched from the blood vessel toward the photophore and exhibits the same type of folding. end, endothelial cell nucleus. Scale bars: 1 μm .

Figure 17. Schematic drawings of the maxilliped. Top: the limb flexed, with the photophores tilting anteriorly as the ligament pulls their apices posteriorly. Middle: the maxilliped in its resting position with the photophores directed downward. Bottom: the limb extended, with the photophores tilted posteriorly as the ligament pushes their apices anteriorly. In each case, light would be directed ventrally with respect to the animal. Scale bar: 2 mm.

Figure 18. High-power light micrograph of the distal tip of the maxilliped showing early stages in the development of several photophores in the main row. In some, refractile droplets are forming in the photocytes (black arrowheads). In slightly older photophores (white arrowheads), larger droplets are surrounded by the carotenoid pigment cell sheath. di, distal; do, dorsal. Scale bar: 150 μm .

Figure 19. Light micrograph of a lateral view of a maxilliped showing the row of photophores at the ventral surface, all oriented in the same direction (tilted slightly posteriorly). Note the small (*i.e.*, developing) photophores (arrowheads) between more mature neighbors. di, distal; do, dorsal. Scale bar: 400 μm .

Figure 20. Light micrograph of a longitudinal section through the maxilliped of *S. debilis* showing two photophores. The larger (and more mature) photophore (arrow) has a photocyte with a large, moderately electron-dense "clear area" (ca) and a relatively small nucleus (pn). The photocyte of the smaller (and younger) photophore (double arrow) has a larger nucleus and a small clear area growing as an electron-lucent droplet within the supranuclear cytoplasm of the cell. cut, cuticle; di, distal; do, dorsal; e, "window" epidermis; l, ligament; p, carotenoid pigment cell processes; r, reflecting pigment cell cap. Scale bar: 40 μm .

Figure 21. Electron micrograph of a very young photocyte in a simple photophore of *S. debilis*. The small clear area droplet (ca) within the cytoplasm lies above the nucleus (pn). A few carotenoid pigment cell processes (p) surround the photocyte, but neither the cap of reflecting pigment cell processes nor the paracrystalline bodies are present at this stage. Scale bar: 3 μm .

maxilliped was amputated at the mid-propodus level and placed on its side on a layer of Sylgard in a petri dish. It was fixed in position by one pin on either side of the propodus and another on the dorsal side of the dactylus so that the two segments were in line. The dactylus was then displaced ventrally (*i.e.*, flexed) with a pin and the preparation was observed through a binocular microscope. As the dactylus was alternately extended and flexed, the photophores tilted in synchrony, first backwards and then forwards. In addition, live juveniles were pinned so that they lay horizontally but were otherwise free to move all their limbs and abdomen. The maxillipeds were placed under a dissecting microscope and their movements were videotaped. Dactyli of the maxillipeds were occasionally flexed, and the orientations of the photophores in them were compared with those in the extended limb. Similar changes in orientation of the photophores were noted.

To obtain an indication of the possible range of photophore tilt angles, we measured the angle between the normal to the cuticular surface and the long axis of the photophore in 14 fixed specimens. Photophores that had a forward tilt (towards the distal end of the limb) due to joint flexion had a maximum angle of about $+31^\circ$ from the normal. Photophores tilted backwards (due to joint extension) measured a maximum of about -42° from the normal. These results provide the first evidence for a form of photophore tilt control that does not depend on a special muscle attached to each organ. In this case the photophores are displaced passively by movements of the joint using an automatic mechanism that ensures that all photophores in the row move in synchrony. A similar system produces rotation of the abdominal photophores of euphausiids (Hardy, 1964); however, in that case, muscles are involved in displacing the ligament.

The development of the photophores in the maxilliped

The sequence of photophore development in *S. debilis* was fully described by Kemp (1910a), who reported that the maxilliped photophores appear at the first postlarval stage. He did not distinguish the development of separate photophore units within the maxilliped dactylus; we have examined similar early postlarvae and found that in all cases there are two small photophores at the distal tip and three at the proximal end. The photophores in the proximal group form the first of those that are associated with the ligament, and contribute to the main row. The distal group remains independent of the ligament. During later development, photophores appear between the two original groups as a linear array (Fig. 18), while both the distal and (more obviously) the proximal groups add more photophores so that they become several photophores wide.

The spacing of photophores within the main row is fairly irregular, and new photophores develop in the gaps between existing ones (Fig. 19). The photophore precursor cells have not been identified, but they are likely to arise from the epidermis where mitotic figures are often found. The first visible sign that a new photophore is developing is the appearance of a differentiating photocyte (Fig. 18). A single refractile droplet appears within this cell and expands within the cytoplasm dorsal to the nucleus, increasing the total cell volume and resulting in the elongation of the cell dorsally (Fig. 20) to form the "clear area" (Dennell, 1940) of the photocyte. The rest of the cytoplasm—containing ribosomes, vesicles, and cytoskeletal elements—becomes restricted to the periphery of the cell (Fig. 21), with abundant mitochondria in the basal cytoplasm ventral to the nucleus. The electron-dense apical paracrystalline bodies are absent from the youngest photocytes (Fig. 21) and appear only as the cell matures.

While these cytoplasmic changes are taking place, nuclear changes are also occurring. At first the nucleus of the developing photocyte is indistinguishable from those of the epidermal cells around it (ovoid and hyperchromatic). Gradually the nucleus acquires the pale and more homogeneous appearance characteristic of the mature photocyte and assumes its lens-like plano-convex shape (Fig. 4).

The growth of the photocytes occurs within a sheath of the processes of the carotenoid pigment cells (Fig. 21). Inspection of serial sections through a number of differentiating photophores showed that photophores that had a reflecting cap always had a carotenoid pigment cell coat, but those that had a coat of carotenoid pigment sometimes lacked a reflecting cap. Thus the reflecting pigment cell presumably differentiates after the carotenoid pigment cell.

Examination of many fully differentiated photophores revealed significant variations in the appearance of the photocyte. In newly formed photophores the clear area is of uniform appearance and lacks any inclusions; more mature photophores contain non-membrane-bound droplets that may completely fill the "clear area," with an accumulation of electron-dense material between them (Fig. 22). These anatomical changes are accompanied by a change in the consistency of the clear area. Sectioning for transmission electron microscopy reveals that the fixed material becomes harder, and this portion of the cell often falls out of sectioned material. The extent of the modification to the clear area varies from photophore to photophore. The simplest interpretation of these observations is that the changes are part of maturation, and that those photophores with the greatest accumulation of material are the oldest. This maturation process seems to occur earlier in *S. debilis* than in *O. spinosus*, because even

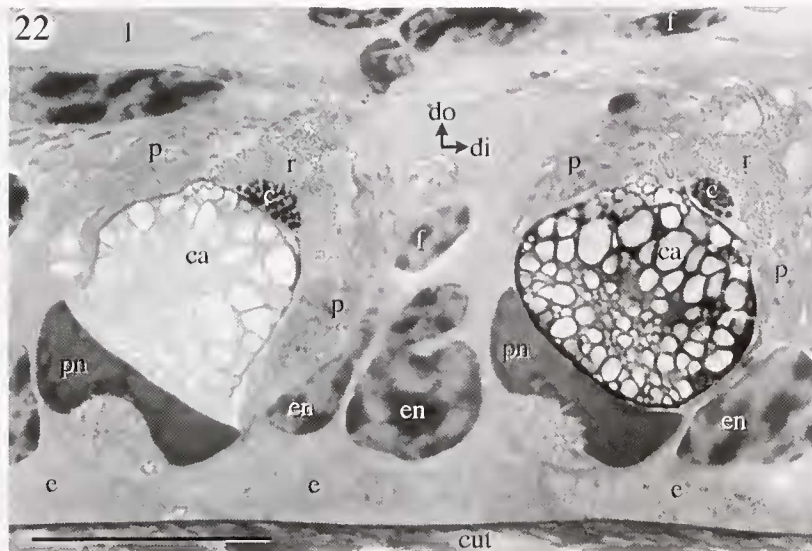


Figure 22. Light micrograph of a longitudinal section through the maxilliped of *Oplophorus spinosus* showing photophores in which the "clear areas" (ca) of the photocytes exhibit stages of increasing osmiophilicity. c, paracrystalline bodies; cut, surface cuticle; di, distal; do, dorsal; e, "window" epidermis cytoplasm; en, "window" epidermis nucleus; f, fibroblast; l, ligament; p, carotenoid pigment cell processes; pn, photocyte nuclei; r, reflector pigment cell cap. Scale bar: 40 μ m.

young photophores of *S. debilis* invariably have darkened "clear areas" (Figs. 20 and 21). This is consistent with the earlier development of the blue cuticular pigment in *S. debilis*.

Pleopod photophores

Each pleopod has a cuticular photophore located in the distal coxa (Fig. 23). It is situated anterior and slightly lateral to the origin of the more distal segments of the pleopod. Externally, its lens is visible as an ovoid region of modified cuticle in which the long axis is more or less transverse with respect to the animal. The convex surface of the lens is surrounded on three sides (anterior, lateral, and medial) by a furrow, the cuticle of which is attenuated; this folded surface acts as a hinge that enables the photophore to be rotated.

Kemp (1910b) described the photophores on the pleopods as the most highly developed. Our studies have shown that, despite their relative complexity, these photophores are composed of the same cell types found in the single-unit (*i.e.*, maxilliped) photophores. They include photocytes, reflecting pigment cells, and carotenoid pigment cells. Most of our observations of pleopod photophores were made on *O. spinosus*, and the general structure of these photophores is summarized in Figure 24.

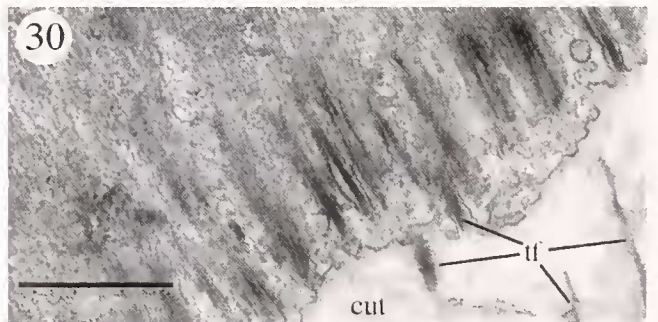
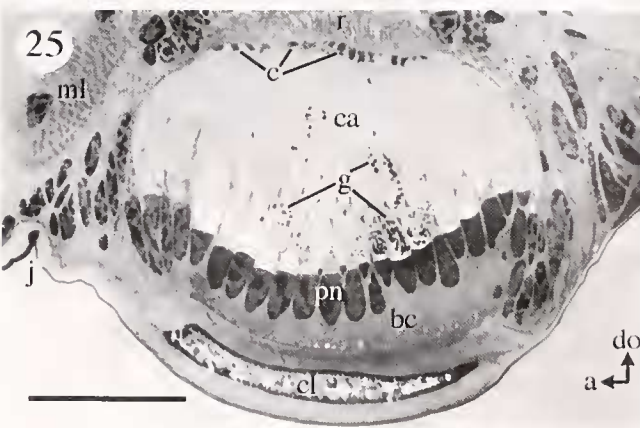
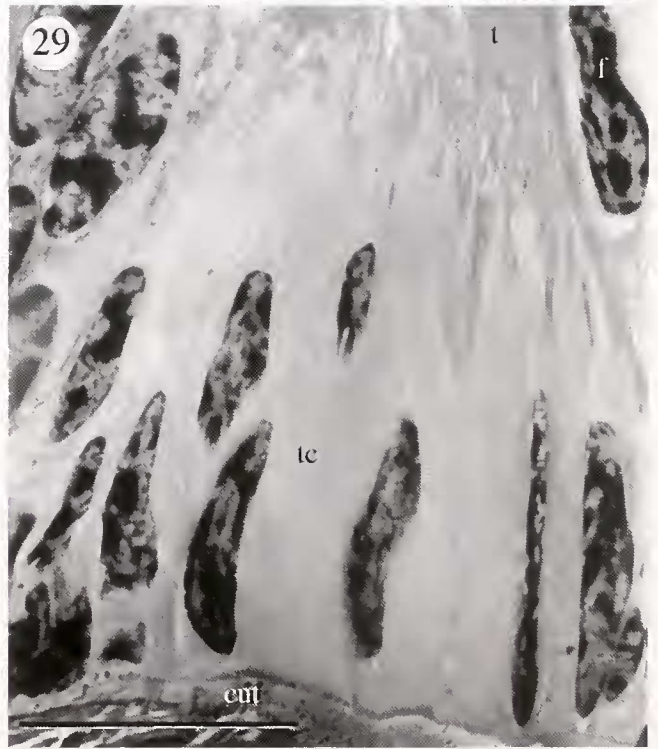
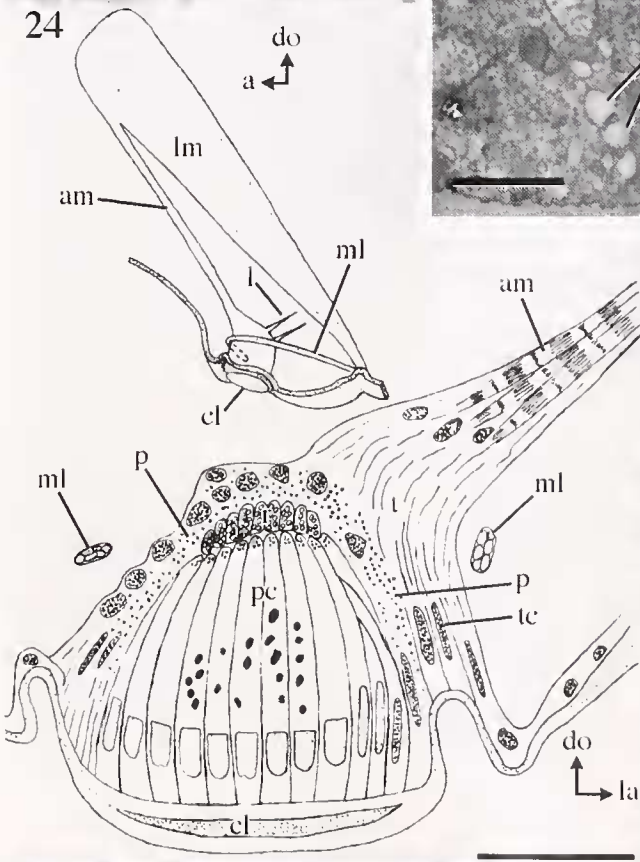
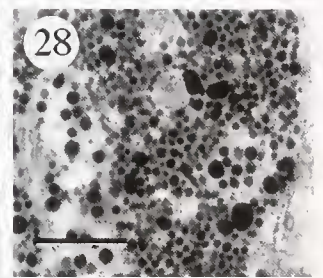
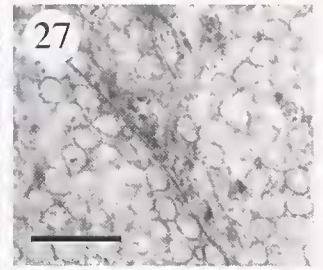
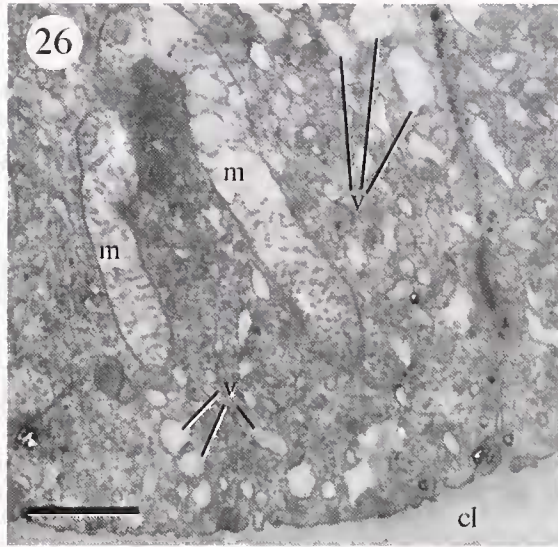
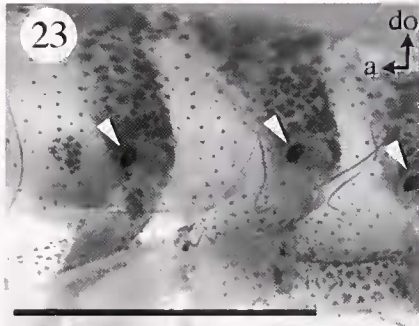
The cuticle covering the photophore forms a concavo-convex lens that in mature specimens is trilaminar (Fig. 25) (Kemp, 1910b; Dennell, 1940). Whereas the photocytes in the simple photophores of the maxilliped are

separated from the cuticle by a layer of epidermis, in the pleopod photophore the photocytes are attached directly to the cuticle and it must be concluded that they secrete the lens structure. The cuticle peripheral to the lens is thinner and often folded (Fig. 25), allowing the cuticular lens to be displaced during photophore tilting movements (see below). This is in contrast to the situation in the maxilliped photophores where the cuticle remains stationary during photophore rotation.

The photocyte

The photocytes of the pleopod photophores are very elongate and somewhat conical (Figs. 24 and 25). The basal cytoplasm lying between the nucleus and the cuticular lens is filled with small, electron-lucent vesicles and a few mitochondria (Fig. 26). These vesicles may contribute to the optical properties of the photophore, or they may simply be related to the secretion or resorption of the cuticle. There are similarities between this portion of the photocyte cytoplasm and the cytoplasm of the specialized window epidermis under the maxilliped photophores—both have abundant vesicles and a few mitochondria, although the vesicles in the pleopod photocytes are smaller and separated by a granular cytoplasm. The similarities of appearance may indicate similarities of function.

The nuclei of the photocytes resemble those of the single-unit maxilliped photophores in that they are pale-staining with diffuse chromatin, have a plano-convex



shape, and often possess a dimple in the distal surface. One difference is in the ratio of length to width: in the pleopod photophores, the photocyte nuclei are about twice as long as they are wide ($\approx 25\text{--}35\ \mu\text{m} \times 12\text{--}15\ \mu\text{m}$), whereas the relationship is reversed in the maxilliped ($\approx 15\ \mu\text{m} \times 30\text{--}35\ \mu\text{m}$). Consequently, the photocyte nuclear layer is thicker in the pleopod photophores than in those of the maxilliped.

The cytoplasm above the nuclei is almost completely occupied by a clear area devoid of organelles, as it is in the maxilliped photocytes. The rest of the cytoplasm is restricted to the periphery of the cell. Membrane-bound paracrystalline bodies in the pleopod photophore are similar in location (at the apex of each of the photocytes) and substructure (a regular square lattice) to those in the maxilliped photophores.

Pigment cells

In the pleopod photophore, the processes of the reflecting pigment cells form a common cap around the apex of the complete set of photocytes (Figs. 24 and 25); in contrast, in the photophores of the maxilliped, each individual photocyte has its own cap of reflecting pigment cell processes. The processes of the carotenoid pigment cells form a sheath peripheral to this reflecting cap. The

sheath covers the photophore down to its base at the level of the integument. Kemp (1910b) suspected the presence of such a pigment coat but was unable to demonstrate it definitively. In *O. spinosus*, the pigment granules in these two types of pigment cell closely resemble those in the maxilliped photophores in appearance and staining properties: the reflecting pigment granules are membrane-bound and electron-lucent, while the carotenoid pigment granules are not membrane-bound and are very electron-dense. Although the reflecting pigment granules are similar in size (up to $0.35\ \mu\text{m}$ in diameter) to those in the maxilliped photophores, the carotenoid pigment granules are larger in the pleopod photophores (up to $0.25\ \mu\text{m}$ in diameter) (Figs. 27 and 28). No observations were made of pigment granule sizes in *S. debilis*.

The musculature and tendon apparatus

Observations of living preparations showed that the photophore can articulate about its anterior margin (see Figs. 31 and 32). Each pleopod photophore has its own anatomically separate mechanism for tilting (unlike the linked arrangement in the maxilliped), and the anatomical findings show that the photophores are controlled by muscles rather than by passive movements of a joint structure as they are in the maxilliped. There are two major muscle

Figures 23–30. Views of pleopod photophores of *Oplophorus spinosus*.

Figure 23. Micrograph of a lateral view of the abdomen showing three of the pleopods with the photophores (arrowheads) visible through the transparent abdominal pleura. a, anterior; do, dorsal. Scale bar: 5 mm.

Figure 24. Semi-schematic drawings showing the arrangement of muscles (upper) and the cellular organization (lower) of the pleopod photophores. The lower is viewed from the medial side; the section is in the transverse of the shrimp. The pleopod is directly influenced by the main longitudinal photophore muscle (lm), the accessory longitudinal muscle (am), and the photophore muscle loop (ml). Short ligaments (l) connect the posterior side of the photophore to the cuticle. The accessory longitudinal muscle is connected to the antero-lateral margin of the photophore by a tendon (t) inserted into tendinous cells (tc). Photogenic cells (pc) are attached basally to the cuticular lens (cl), and the apices of these cells are capped by processes of reflecting pigment cells (r). Processes of carotenoid pigment cells (p) ensheath the photophore. a, anterior; do, dorsal; la, lateral. Dimensions are approximate. Scale bar for section: $100\ \mu\text{m}$.

Figure 25. Light micrograph through a photophore. The photocytes are arrayed in rows above the trilaminar cuticular lens (cl) with their nuclei (pn) above a basal cytoplasm (bc) and below a clear area (ca). Each photocyte contains paracrystalline bodies (c) at the apex of its clear area; in the center of the photophore, many photocytes have accumulated dark granules (g) in the clear areas. The processes of reflecting pigment cells (r) form a cap above the photophore. The pleopod photophore articulates around a thin, cuticular hinge joint (j). a, anterior; do, dorsal. Scale bar: $100\ \mu\text{m}$.

Figure 26. Electron micrograph of the basal cytoplasm of the photocytes. The cytoplasm is filled with numerous membrane-bound vesicles (v) and contains a few mitochondria (m). cl, cuticular lens. Scale bar: $1\ \mu\text{m}$.

Figure 27. Electron micrograph of reflecting pigment cell processes filled with membrane-bound pigment granules. Scale bar: $1\ \mu\text{m}$.

Figure 28. Electron micrograph of a carotenoid pigment cell filled with dark granules. Scale bar: $1\ \mu\text{m}$.

Figure 29. Light micrograph of the lateral margin of a photophore. Tendinous cells (tc) form a sheet that is attached at its base to the cuticle (cut); the articulating tendon (t) of the photophore inserts into the apex of these cells. f, fibroblast. Scale bar: $40\ \mu\text{m}$.

Figure 30. Electron micrograph through tendinous cells of the photophore at their junction with the cuticle (cut). The cytoplasm of these cells is loaded with microtubules oriented perpendicular to the cuticular surface. Tonofibrillae (t) anchor the tendinous cells to the cuticle. Scale bar: $1\ \mu\text{m}$.

sets: a pair of longitudinal muscles concerned with backward rotation of the photophore, and a muscle loop that tilts the photophore forward. The former have their origin on the antero-lateral wall of the coxa dorsal to the photophore. The larger of the two muscles (the main longitudinal muscle) inserts onto the cuticle of the coxa about 0.5 mm posterior to the photophore (Fig. 24). The smaller longitudinal muscle (the accessory longitudinal muscle) arises as a branch of the larger one and runs directly to the photophore itself, inserting into the antero-lateral margin of the photophore by means of a tendon.

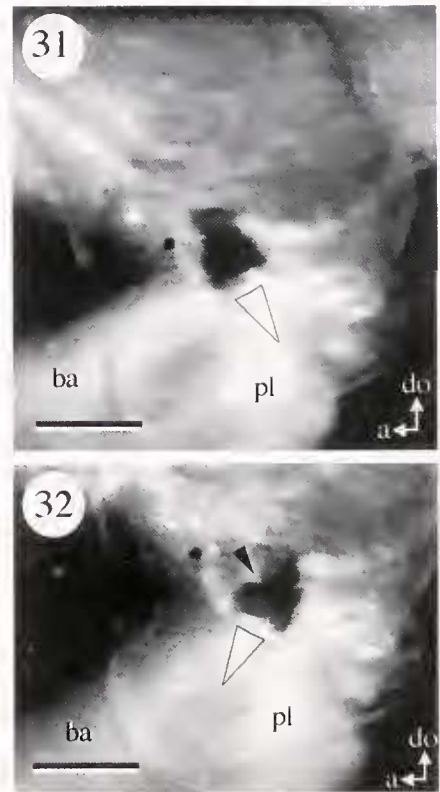
This description differs significantly from that of Dennell (1940), who described only the accessory longitudinal muscle (his "longitudinal photophore muscle") and not the main longitudinal muscle. We do confirm the presence of Dennell's (1940) "photophore muscle loop," which passes around the anterior side of the photophore. One end of the loop inserts outside the cuticular groove that surrounds the photophore, and the other end inserts medially into an invagination of the cuticle at the site where the main longitudinal muscle described above terminates. In addition to these muscles, there is a set of several short ligaments that attach the posterior region of the photophore to the adjacent wall of the coxa (Fig. 24).

Of the various muscles, only the accessory longitudinal muscle is connected directly to the photophore. The tendon that joins the muscle to the photophore is composed of fibrils that have the same dimensions and periodicity as do those making up the ligament that controls tilt in the row of maxilliped photophores. They are produced by fibroblasts found within the tendon (Fig. 29). Bundles of fibrils insert into the apices of a strip of modified epidermal, or "tendinous," cells (Mellon, 1992) at the antero-medial perimeter of the photophore (Figs. 29 and 30).

The cytoplasm of the tendinous cells is densely filled with microtubules oriented perpendicular to the cuticle. The base of each tendinous cell is firmly fixed onto the inner face of the cuticle by means of tonofibrillae that penetrate the layers of cuticle externally and extend into invaginations of the tendinous cells internally (Fig. 30). The attachment of cells to cuticle in this way has been described in various crustaceans such as shrimps (Talbot *et al.*, 1972) and crayfish (Jahromi and Atwood, 1976, 1977), as well as in insects (Lai-fook, 1967). The lateral margins of adjacent attachment cells are often strongly interdigitated.

Tilting behavior

The arrangements described above provide an anatomical basis for the observable tilting behavior of this type of photophore. Contraction of the main longitudinal muscle would result in backward rotation of the cuticular lens about the hinge anterior to it. There is no obvious antago-



Figures 31 and 32. Images from a videotaped sequence of an *Ophiophorus spinosus* juvenile, showing a photophore on the coxa of a pleopod tilted in different orientations: posteriorly in Fig. 31 and anteriorly in Fig. 32. The basis of the pleopod (ba), as well as the photophore itself, is visible beneath the abdominal pleura (pl). The open arrowheads indicate the tilt direction. Note the kink in the anterior face of the pleopod in Fig. 32, which is caused by contraction of the photophore muscle loop (black arrowhead). a, anterior; do, dorsal. Scale bars: 1 mm.

nistic muscle set and it is assumed that when the main longitudinal muscle relaxes, elasticity of the cuticle returns it to its former position. The function of the accessory longitudinal muscle may be to maintain tension on the photophore when the main longitudinal muscle contracts. This would be necessary to keep the photophore pointing in the appropriate direction during movements of the lens. The short ligaments would provide support for the photophore during this process. The anatomical arrangement of the loop muscle means that its contraction would rotate the photophore forwards by pulling on its anterior margin.

To obtain information on tilting behavior, juvenile specimens of both *O. spinosus* and *S. debilis* were restrained and videotaped from the side, as described earlier. Three types of movement were noted: (1) frequent small twitches (approximately 4°), (2) relatively large rotations in which the posterior margin of the photophore was raised to rotate the photophore backwards by as much as -40° from the resting position (Fig. 31), and (3) rela-

tively large rotations in which the anterior wall of the photophore was pulled posteriorly (by the photophore muscle loop) to rotate the photophore to point forward by as much as $+46^\circ$ (Fig. 32). None of these types of movement appears to be related to any aspect of pleopod beating, which involves movements of only those parts of the limb that are distal to the photophore. Observations of videotape sequences showed that the photophores in adjacent segments often but not always rotated similarly and simultaneously, even though the pleopod photophores are anatomically independent from each other. The larger rotations were sometimes but not always associated with flexion of the abdomen. However, forcible flexion of the abdomen did not always induce rotation.

Growth and development

Kemp (1910a) reported that the pleopod photophores of *S. debilis* are present in the first zoea. The photophores in the pleopods of young postlarvae are extremely small, and mid-longitudinal sections of the organ are just a few photocytes wide (Fig. 33). In older shrimps they are much larger, and they can be up to 20 cells wide. The total number of photocytes has been estimated to be over 300 in fully developed photophores (Kemp, 1910b). Growth of the photophore appears to involve the differentiation

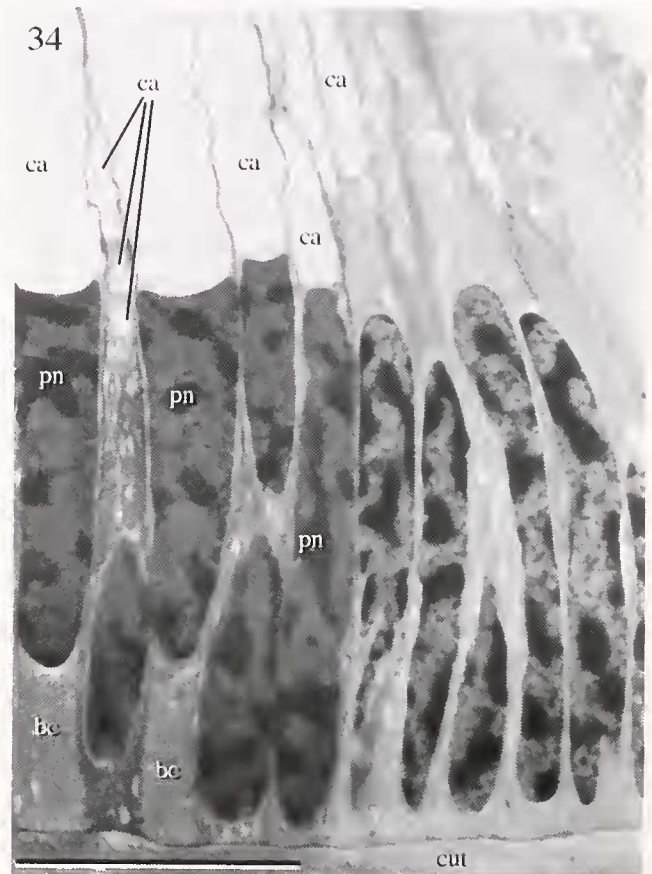


Figure 34. Light micrograph at the growing edge of the pleopod photophore of *Oplophorus spinosus*, where undifferentiated epidermal cells are developing the features of mature photocytes, including the formation of a clear area (ca), lens-shaped, homogeneous nuclei (pn), and vesiculated basal cytoplasm (bc), cut, cuticle. Scale bar: $40\ \mu\text{m}$.

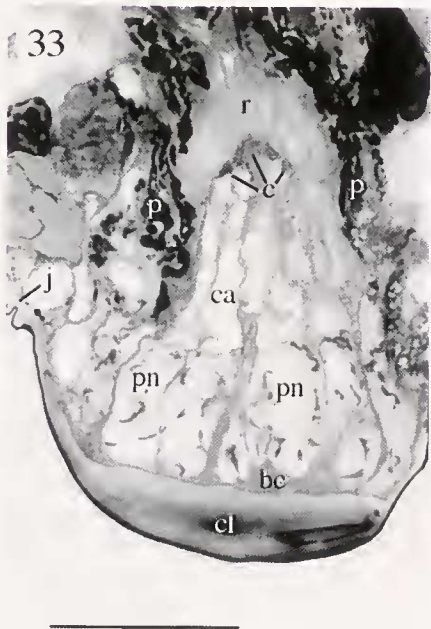


Figure 33. Light micrograph through the pleopod photophore of a postlarval specimen of *Oplophorus spinosus*. The photophore exhibits all the features of the adult organ. bc, basal cytoplasm of photocytes; c, paracrystalline bodies; ca, clear area; cl, cuticular lens; j, articulating joint; p, carotenoid pigment cell processes; pn, photocyte nuclei; r, reflecting pigment cell cap. Scale bar: $40\ \mu\text{m}$.

of immature cells at the periphery of the organ (Fig. 34). This conclusion is based on the observation that photocytes at the edge of the photophore are less mature than those in the center: cells at the edge of the photophore lack a clear area, while the extent of the clear area is greatest in photocytes situated away from the margins of the photophore. Furthermore, the clear area in the most centrally located photocytes shows an accumulation of an electron-dense material that seems to increase with maturation.

Events involved in this differentiation process appear to be similar to stages in the development of photocytes in the maxilliped. The first indication that an epidermal cell at the periphery of the photophore is differentiating into a photocyte is the appearance of a clear area above the nucleus of the cell. Next, the clear area enlarges in the differentiating photocyte, which elongates in an apical direction. This is seen in cells located slightly more centrally. Finally, toward the middle of the organ, the shape of the nucleus changes from ovoid to plano-convex, the

nucleoplasm becomes more homogeneous, and the subnuclear cytoplasm assumes the vesiculated appearance of a mature photocyte (Fig. 34). All of these events occur within the sheath of the carotenoid pigment cell layer.

Additional changes take place in older photocytes, found in the center of the photophore. In these cells, the clear area gradually fills almost completely with osmiophilic granules (see Fig. 25), which eventually coalesce. This differs from what occurs in the maxilliped photocytes. In those cells, the clear area fills with electron-lucent droplets and the material between them becomes increasingly osmiophilic (see Fig. 22). As in the maxilliped, however, the maturation process in photocytes of the pleopod is accompanied by a hardening of the cytoplasm, as evidenced by the material becoming difficult to section for electron microscopy.

Discussion

The term "photophore" is normally used to describe a composite structure in which the light-emitting cells (photocytes) are associated with accessory optical structures. Photophores almost invariably contain numerous photocytes. In *S. debilis* and *O. spinosus*, however, this usage of photophore is clearly applicable to the individual units within the 3rd maxilliped dactylus, each of which contains only a single photocyte but which nevertheless also has refractive, reflective, and light-shielding structures. Examination of a variety of photophores (*sensu* Kemp, 1910b) on these animals (M.S.N., unpub. data) shows that, with the sole exception of the pleopod photophores, they are modular structures made up of a variable number of subunits, each of which is equivalent to one of the photophores containing a single photocyte and present in the maxilliped series. A modular arrangement of photophores at such a small scale has not been described in any other animal. In the few other cases known of photophores with only a single photocyte (e.g., the shark *Euprotomicrus* [Hubbs *et al.*, 1967]), the photophores are widely scattered over the ventral surface and not aggregated into specific groups. Modular assemblages (or groups) of larger photophores are, however, typical of many deep-sea fishes and are particularly prominent in the Sternoptychidae (e.g., *Valenciennellus* and the hatchetfishes). They are also present in a number of cephalopods, notably the Ommastrephidae in which the millimeter-sized subunits may form a very large dorsal photophore. The organs of Pesta, the hepatic photophores of species of *Sergestes*, are modular assemblages of specialized liver tubules, each tubule containing many photocytes and reflective cells (Herring, 1981).

The fine structure of the photophores of *S. debilis* and *O. spinosus* is very similar, as was recognized by Kemp (1910b). There are no other examples of cuticular photo-

phores in the genera within the Caridea, but among the Penaeidea they also occur in some species of the sergestid *Sergia*; the solenocerids *Hymenopenaeus*, *Mesopenaeus*, *Hadropenaeus*, and *Solenocera*; and the penaeid *Gennadas* (see Herring, 1985b, for references). Nothing is known of their ultrastructure in any of these genera, but the early histological descriptions of those in *Sergia* (Kemp, 1910b; Terao, 1917) closely resemble those in similar studies of *O. spinosus* and *S. debilis* (Kemp, 1910b; Dennell, 1940). At the ultrastructural level, the most striking parallel with other decapods is in the paracrystalline bodies that provide the photogenic core of the organs in both *O. spinosus* and *S. debilis*. The photocytes of *Sergestes* have similar paracrystalline bodies or platelets, but with a lattice periodicity of 5–8 nm, considerably lower than the 14.8 nm in *O. spinosus*. The presence of paracrystalline material at the photogenic core is not restricted to these decapods but also occurs in euphausiid shrimp, cranchiid and enoploteuthid squids, and the anglerfish *Linophryne*. Its functional significance is not known; other complex lattice structures ("photosomes") characterize the photocytes of polynoid worms.

The pleopod photophores are more complex than mere aggregations of subunits because the photocytes are now arranged radially rather than linearly (as Dennell recognized), and the pigment cells are organized to form a common sheath. This complexity is associated with a rotatory capability. The possibility of rotation of these photophores was first suggested by Kemp (1910b), and a general anatomical arrangement that might allow it was described by Dennell (1940). However, our description differs considerably from that of Dennell. His explanation was presumably limited by the state of preservation of the animals and the difficulties of interpreting structures in wax-embedded specimens. He failed to notice the main longitudinal muscle, and described other muscles that were not present in our material. In addition, he described a photophore nerve. We found no evidence for such a structure and believe that what Dennell identified as a nerve was in fact extracellular fibrils of the tendon and carotenoid pigment cell processes.

The configuration of the muscle loop is highly unusual and actually deforms the photophore during forward rotation. Further observations of live shrimps are necessary before the exact roles of the main and accessory longitudinal muscles can be confirmed.

The organs of Pesta in *Sergestes similis* are also capable of rotation as part of a counterillumination mechanism (Latz and Case, 1982), but the structural basis has not yet been described. It is probable that similar antagonistic muscle and ligament systems are involved. In *S. similis*, angular rotation of up to 140° can be achieved in the plane of pitch and is statocyst-mediated, as was demonstrated by an elegant series of ablation experiments. In

euphausiids, the rotation of the photophores is linked to angular movements of the eyestalks in response to directional changes of incident light (Land, 1980; Grinnell *et al.*, 1988). Simultaneous angular rotations of up to 165° were recorded for both the thoracic and abdominal photophores, and spontaneous small movements of the photophores (15°–30°) took place in eyeless animals. The authors concluded that feedback concerning eye movement is not necessary and that parallel signals from the central nervous system control the photophore positions. Our video observations of restrained specimens were made on animals exposed to room lighting and cannot be interpreted as normal behavior. What they do show are changes in orientation of up to 87°. Whether there is normally an element of visual control over the rotation (as in euphausiids) or whether it is statocyst-mediated (as in *S. similis*) has not been determined.

The rotation of the 3rd maxilliped photophores is quite different in that they are linked to a ligament and rotate in mechanical response to local changes in the relative positions of the propodus and dactylus. This permits rotation only in the plane of pitch. The linking mechanism is very similar to that of the two parallel ligaments responsible for the simultaneous rotation of the abdominal photophores of euphausiids. However, in the latter animals there is some very limited capability for lateral (roll) rotation (Land, 1980; Grinnell *et al.*, 1988), which is clearly not possible in the system controlling the maxilliped photophores. In addition, the ligaments in the euphausiid case are under direct muscular control. We do not know of any rotatory capability in the modular photophores elsewhere on the body of *O. spinosus* or *S. debilis*; it is almost certainly impossible for the carapace photophores but cannot be ruled out for others (*e.g.*, the 5th thoracic limb or posterior streak photophores).

The different means of photophore rotation may have different optical consequences. In the pleopod photophore, the lens is an integral part of the structure and rotates with it during contraction of the longitudinal muscles, so the optical output is unaffected. When the photophore muscle loop contracts, the photophore may be displaced relative to the underlying lens. In the maxilliped, the cuticular lens-like thickening remains fixed in position as the photophores rotate above it. Any optical changes (*e.g.*, lens misalignment) consequent on the different orientation are likely to be small because the thickening runs the length of the dactylus and probably acts as a cylindrical lens so that the photophore output will still pass through it, albeit with an altered angle of incidence.

All evidence indicates that the main role of the photophores in these animals is counterillumination (Herring, 1976). The presence and positions of the photophores on the limbs need to be considered in terms of their normal disposition during swimming. The 3rd maxilliped is held

forwards, almost horizontal, which means that the photophores point more or less downwards within the limits of their movement. Those on the pleopod also point ventrally. However, on other limbs, photophores face in different directions in different organs. Consideration of the ways in which the limbs are folded during swimming shows that even in these cases the photophores point in a predominantly downward direction. The thoracic limbs (pereopods) are folded at the meral/carpal joint so that where the anterior margin of the proximal limb segments faces dorsally, that of the distal segments faces ventrally. This explains why the photophores face opposite sides of the limb in distal (carpus and propodus) and more proximal segments. This apparently paradoxical inversion of the photophores on the propodus of the 5th limb, relative to those of the streak behind the limb, greatly perplexed Dennell (1940), who described it in *Oplophorus* (noting that "the inversion . . . is very surprising and cannot be readily explained") and in *Systellaspis* ("a most astonishing and inexplicable feature"). The consistently ventral direction of photophores at different sites strongly suggests that they have a counterillumination function.

Our description of the cellular architecture of oplophorid photophores is simpler than that of Dennell (1940). He described more cell types than we have identified, but this interpretation was almost certainly due to his use of relatively crude fixatives and wax histology. In addition, he interpreted profiles from different levels of the same type of cell as belonging to different cell classes, a misjudgment that often arose from non-ideal planes of section. For example, Dennell described the photophores of the 5th thoracic limb and in the large luminous streak behind its base as showing succeeding stages of differentiation. However, this appearance is the result of oblique sections (see Fig. 35), as becomes clear if sections of carefully oriented material are compared with oblique sections. Dennell's *S. pellucida* (as *S. affinis*) "photogenic unit 1" (his Fig. 26) is a section through the clear area, surrounded by the processes of the reflecting pigment cap; his "photogenic unit 2" is a section through the middle of the reflecting pigment cap; and "photogenic unit 3" is a section through the top of the cap. His interpretation of the luminous streak in *O. spinosus* (as *H. grimaldii*, his Fig. 15) is even more complicated but equally explicable as an obliquely sectioned organ. "Photogenic cell 1" is a section through the photocyte nucleus, "2" is an oblique section through the base of the clear area and grazing the nucleus, "3" is through the middle portion of the clear area, "4" is through the upper third of the clear area and reflecting cell processes, and "5" is through the apex of the photophore. The "central body" (his Fig. 16) consists of the paracrystalline bodies (elsewhere labeled "basal cap of photogenic cell" and, in the pleopod photophore, "granular zone").

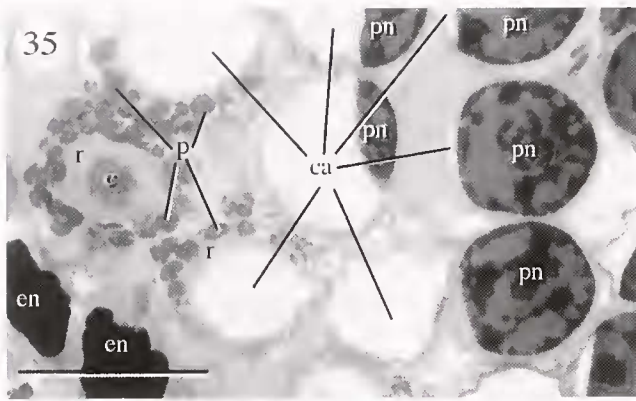


Figure 35. Light micrograph of an oblique section through a group of maxilliped photophores in *Oplophorus spinosus*, which shows the appearance of the photophores at different levels of section. c, paracrystalline bodies; ca, clear area; en, "window" epidermal nuclei; p, carotenoid pigment cell processes; pn, photocyte nuclei; r, reflecting pigment cell processes. Scale bar: 40 μ m.

Dennell (1940) described a fibrous reflector in the pleopod photophores of *O. spinosus*; using electron microscopy, we have found this to be a ligament with associated cell processes of carotenoid pigment cells. He identified the actual reflector as the "striated zone." Nevertheless, Dennell's detailed histological and morphological account is immensely thorough and, if correctly relabeled, provides an invaluable comparative survey.

One unexpected feature of our study of the pleopod photophore is the apparent absence of any identifiable epidermal cells between the photocytes and the lens cuticle, though these are clearly visible as "window" epidermis in the maxilliped photophores. We can only assume that in the pleopod photophores the cuticle is secreted by the photocytes at each molt. The window epidermis structures (small vesicles and few mitochondria) seen also in the basal cytoplasm of the pleopod photocytes suggest that they have a similar function, either in the optics of the photophore or in the secretion of the cuticle. Another surprising feature is the absence of any identifiable direct neural connections to the photophores. Any nerves we have seen have been associated with the muscles. This suggests that light emission is controlled by some indirect mechanism. One possibility is that the circulatory system is involved, as is the case in euphausiids where sphincters control the blood supply to each photophore (Herring and Locket, 1978). Euphausiids, as well as *Oplophorus* and *Systellaspis*, can be induced to luminesce by treatment with low levels of serotonin (5-OH tryptamine). Serotonin also induces luminescence in *Sergestes similis* photophores, and neurohumoral control is implied by the slow induction of bioluminescence by photic stimuli (Latz and Case, 1992; Latz, 1995). Many of the nerves reported by Dennell (1940) were undoubtedly misidentifications of

striated material that were in reality either ligament or pigment cell processes. Nevertheless, we cannot entirely rule out the possibility of some direct neural control, and ventral nerve cord section has produced variable and inconclusive results (Herring, 1976).

The photophores of these shrimps represent an elaborate degree of optical structure on a small scale. The combined output of the many (probably more than a thousand) units over the ventral surface of the body in conjunction with the animal's swimming movements would provide extremely effective counterillumination, probably well beyond the resolution of the eye of a predator. The ability of the photophores to rotate in (presumed) response to changes of the animal's orientation in the water affords an additional refinement to the camouflage capability. Comparisons of fine structure between these photophores and the cuticular photophores of other decapods, particularly species of *Sergia*, are highly desirable. Even more valuable would be direct observations of the behavior of the photophores with respect to the activity of the shrimps.

Acknowledgments

This study was supported by NERC grants GR9/0119A to PMJS and GR3/11212 to PMJS and PJH. MSN gratefully acknowledges a CAFR grant from Providence College, and is grateful for the assistance of Dr. Edward A. Gaten and the staff of the Electron Microscopy Suite of the University of Leicester.

Literature Cited

- Ball, E. E., J. C. Kao, R. C. Stone, and M. F. Land. 1986. Eye structure and optics in the pelagic shrimp *Acetes sibogae* (Decapoda, Natantia, Sergestidae) in relation to light-dark adaptation and natural history. *Phil. Trans. R. Soc. B* 313: 251–270.
- Contière, H. 1905. Note préliminaire sur les *Eucyphotes* recueillis par S.A.S. le Prince de Monaco. *Bull. Mus. Oceanogr. Monaco* 48: 1–35.
- Contière, H. 1906. Notes sur la synonymie et le développement de quelques Hoplophoridae. *Bull. Mus. Oceanogr. Monaco* 70: 1–20.
- Dennell, R. 1940. On the structure of the photophores of some decapod Crustacea. *Discovery Rep.* 20: 307–381.
- Dennell, R. 1942. Luminescence in decapod Crustacea. *Sci. J. Roy. Coll. Sci.* 12: 60–68.
- Dennell, R. 1955. Observations on the luminescence of bathypelagic Crustacea Decapoda of the Bermuda area. *J. Linn. Soc. Zool.* 42: 393–406.
- Denton, E. J., J. B. Gilpin-Brown, and P. G. Wright. 1972. The angular distribution on light produced by some mesopelagic fish in relation to their camouflage. *Proc. R. Soc. Lond. B* 182: 145–158.
- Denton, E. J., P. J. Herring, E. A. Widder, M. I. Latz, and J. F. Case. 1985. The roles of filters in the photophores of oceanic animals and their relation to vision in the oceanic environment. *Proc. R. Soc. Lond. B* 225: 63–97.
- Doughtie, D. G., and K. R. Rao. 1984. Ultrastructure of the eyes of the grass shrimp, *Palaemonetes pugio*. General morphology, and light and dark adaptation at noon. *Cell Tiss. Res.* 238: 271–288.

- Elofsson, R. 1971.** The ultrastructure of the chromatophores of *Crangon* and *Pandalus* (Crustacea). *J. Ultrastruct. Res.* **36**: 263–270.
- Grinnell, A. D., P. M. Narins, F. T. Awbrey, W. M. Hamner, and P. P. Hamner. 1988.** Eye/photophore co-ordination and light-following in krill, *Euphausia superba*. *J. Exp. Biol.* **134**: 61–77.
- Hardy, M. G. 1962.** Photophore and eye movement in the euphausiid *Meganyctiphanes norvegica* (G. O. Sars) *Nature* **196**: 790–791.
- Hardy, M. G. 1964.** The rotary mechanism and innervation of the abdominal photophores of the euphausiid crustacean *Meganyctiphanes norvegica*. *J. Physiol. Lond.* **173**: 16P–18P.
- Harvey, E. N. 1952.** *Bioluminescence*. Academic Press, New York.
- Hastings, J. W., and J. G. Morin. 1991.** Bioluminescence. Pp. 131–170 in *Neural and Integrative Animal Physiology*. C. L. Prosser, ed. Wiley-Liss, New York.
- Herring, P. J. 1973.** Depth distribution of the carotenoid pigments and lipids of some oceanic animals. 2. Decapod crustaceans. *J. Mar. Biol. Assoc. U.K.* **53**: 539–562.
- Herring, P. J. 1976.** Bioluminescence in decapod Crustacea. *J. Mar. Biol. Assoc. U.K.* **56**: 1029–1047.
- Herring, P. J. (ed.) 1978.** *Bioluminescence in Action*. Academic Press, London.
- Herring, P. J. 1981.** The comparative morphology of hepatic photophores in decapod Crustacea. *J. Mar. Biol. Assoc. U.K.* **61**: 723–737.
- Herring, P. J. 1985a.** How to survive in the dark: bioluminescence in the deep sea. Pp. 323–350 in *Physiological Adaptations of Marine Animals*, M. S. Laverack, ed. *Symp. Soc. Exp. Biol.* **39**.
- Herring, P. J. 1985b.** Bioluminescence in the Crustacea. *J. Crust. Biol.* **5**: 557–573.
- Herring, P. J., and J. A. Locket. 1978.** The luminescence and photophores of euphausiid crustaceans. *J. Zool., London.* **186**: 431–462.
- Huhbs, C. L., T. Iwai, and K. Matsubara. 1967.** External and internal characters, horizontal and vertical distribution, luminescence and food of the dwarf pelagic shark *Euprotomicrus bispinatus*. *Bull. Scripps Inst. Oceanogr.* **10**: 1–64.
- Jahromi, S. S., and H. L. Atwood. 1976.** Attachments of phasic and tonic abdominal extensor muscles in crayfish. *Can. J. Zool.* **54**: 1256–1269.
- Jahromi, S. S., and H. L. Atwood. 1977.** Normal organization and induced degeneration of the muscle attachment in the crayfish opener muscle. *Can. J. Zool.* **55**: 825–835.
- Karnovsky, M. J. 1965.** A formaldehyde-glutaraldehyde fixative of high osmolality for use in electron microscopy. *J. Cell Sci.* **27**: 137A–138A.
- Kemp, S. 1910a.** The Decapoda Natantia of the coast of Ireland. *Fisheries, Ireland, Sci. Invest. (1908)* **1**: 3–190.
- Kemp, S. 1910b.** Notes on the photophores of decapod Crustacea. *Proc. Zool. Soc. Lond.* **11**: 639–651.
- Lai-fook, J. 1967.** The structure of developing muscle insertions in insects. *J. Morphol.* **123**: 503–527.
- Land, M. F. 1980.** Eye movements and the mechanism of vertical steering in euphausiid crustacea. *J. Comp. Physiol.* **137**: 256–265.
- Latz, M. I. 1995.** Physiological mechanisms in the control of bioluminescent countershading in a midwater shrimp. *Mar. Fresh. Behav. Physiol.* **26**: 207–218.
- Latz, M. I., and J. F. Case. 1982.** Light organ and eyestalk compensation to body tilt in the luminescent midwater shrimp, *Sergestes similis*. *J. Exp. Biol.* **98**: 83–104.
- Latz, M. I., and J. F. Case. 1992.** Slow photic and chemical induction of bioluminescence in the midwater shrimp *Sergestes similis* Hansen. *Biol. Bull.* **182**: 391–400.
- Martin, G. G., and J. E. Hose. 1992.** Vascular elements and blood (hemolymph). Pp. 117–146 in *Microscopic Anatomy of Invertebrates*. Vol. 10: *Decapod Crustacea*. F. W. Harrison and A. G. Humes, eds. John Wiley, New York.
- Mellon, D. 1992.** Connective tissue and supporting structures. Pp. 77–116 in *Microscopic Anatomy of Invertebrates*. Vol. 10: *Decapod Crustacea*. F. W. Harrison and A. G. Humes, eds. John Wiley, New York.
- Peterson, D. R., and R. F. Loizzi. 1974.** Ultrastructure of the crayfish kidney—coelomosae, labyrinth, and nephridial canal. *J. Morphol.* **142**: 241–263.
- Piekos, W. B. 1986.** The role of reflecting pigment cells in the turnover of crayfish photoreceptors. *Cell Tiss. Res.* **244**: 645–654.
- Roe, H. S. J., and D. M. Shale. 1979.** A new multiple rectangular midwater trawl (RMT1 + 8M) and some modifications to the Institute of Oceanographic Sciences' RMT1 + 8. *Mar. Biol.* **50**: 217–236.
- Schönenberger, N. 1977.** The fine structure of the compound eye of *Squilla mantis* (Crustacea, Stomatopoda). *Cell Tiss. Res.* **176**: 205–233.
- Shelton, P. M. J., E. Gaten, and C. J. Chapman. 1986.** Accessory pigment distribution and migration in the compound eye of *Nephrops norvegicus* (L.) (Crustacea: Decapoda). *J. Exp. Mar. Biol. Ecol.* **98**: 185–198.
- Talbot, P., W. H. Clark, and A. L. Lawrence. 1972.** Ultrastructural observations of the muscle insertion and modified branchiostegite epidermis in the larval brown shrimp, *Penaeus aztecus*. *Tissue Cell* **4**: 613–628.
- Terao, A. 1917.** Notes on the photophores of *Sergestes prehensilis* Bate. *Annot. Zool. Jpn.* **9**: 299–316.
- Wild, R. A., E. Darlington, and P. J. Herring. 1985.** An acoustically controlled cod-end system for the recovery of deep-sea animals at *in situ* temperatures. *Deep-Sea Res.* **32**: 1583–1589.